

## Contamination-induced particle production during balloon flights: Origin for unexpected ice particle observations in the Arctic?

Cornelius Schiller<sup>1</sup>, Terry Deshler<sup>2</sup>, and Thomas Peter<sup>3</sup>

**Abstract.** Stratospheric air in the vicinity of a balloon payload have been found to be contaminated with H<sub>2</sub>O mixing ratios of 10-80 ppmv during ascent, float, and slow descent at altitudes above 20 km. The contamination appeared in brief events often coincident with the occurrence of micron-sized particles and with increased temperatures. The observed H<sub>2</sub>O mixing ratios may result in ice particle production within 10-60 s in the lower stratosphere, even at temperatures around 200 K, i.e. well above the frost point of the ambient air. Thus, plumes of H<sub>2</sub>O-contaminated air must be seriously considered as an explanation for balloon-borne observations in the past, which have been interpreted as apparent thin layers of large ice particles above the frost point. These possible artifacts reduce the weight of evidence for NAT-coated ice particles in the stratosphere at temperatures above the frost point.

### Introduction

During a balloon flight on 920127 (yyymmdd format) from Kiruna, Sweden (68°N), particles with radii  $r \geq 5 \mu\text{m}$  were detected in burst-like events at altitudes between 19 and 24 km and were interpreted as thin ice particle layers [Deshler *et al.*, 1994]. Within altitude intervals of 30-50 m, corresponding to the 0.1 Hz sampling frequency, concentrations of large particles changed by several orders of magnitude. These observations were made during ascent in daylight. Descent measurements were not available due to instrument failure. The origin and existence of such large particles is a mystery. Calculations of the condensed mass indicated water vapor mixing ratios of 0.5-6.0 ppmv in the most prominent particle events, which was found to be consistent with Arctic stratospheric water vapor measurements of 5.5-6.0 ppmv in this altitude range. This led Deshler *et al.* to suggest that the particles were ice even though the air temperature was 5-10 K above the frost point, defined as the maximum temperature at which ice can exist in equilibrium with the available gas phase H<sub>2</sub>O. The interpretation was further complicated by temperature oscillations displaying peak-to-peak amplitudes of 5-10 K in the altitude range of the particle observations. Particle events between 20 and 24 km were positively correlated with temperature. During a nighttime balloon flight 7 hours prior to these observations, Khattatov *et al.* [1994] also found aerosol events at the same altitudes, but scattering ratios were not indicative of ice. Other so-called micro-layers of particles have been reported from the Arctic on 890130 [Hofmann and Deshler, 1989], containing particles with

maximum radii of 2-3  $\mu\text{m}$  and therefore much lower mass mixing ratios. These layers have been interpreted as NAT particles [Hofmann, 1990], but they might possibly be related to the contamination phenomenon reported below.

Based on a mesoscale mountain-wave model and microphysical studies, Peter *et al.* [1994] suggested that ice clouds had formed in lee waves over the Norwegian mountains 200-300 km upwind of the observations on 920127. In an attempt to explain Deshler *et al.*'s observations of large particles above the frost point, they suggested that ice particle lifetimes might have been prolonged due to a coating of nitric acid trihydrate (NAT). Evidence for the existence of stratospheric ice crystals which contain nitrate ions and apparently survive longer in an environment subsaturated with respect to ice has been provided by airborne measurements [Goodman *et al.*, 1997]. Middlebrook and Tolbert [1996] found in laboratory studies, using fast thermal desorption, that ice coated with nitric acid trihydrate evaporated at temperatures about 4 K higher than uncoated ice. Biermann *et al.* [1998] showed in thermodynamic laboratory experiments that a thin (10-100 nm) NAT coating is not capable of protecting an underlying macroscopic ( $\varnothing \approx 1 \text{ cm}$ ) ice layer against evaporation, even if temperatures are only marginally (0.2 K) above the ice point. The latter thermodynamic experiment is not in contradiction with the kinetic measurement by Middlebrook and Tolbert, but puts it in perspective by suggesting that a NAT coating can at most lead to a slight prolongation of the ice lifetime. The applicability of these macroscopic experiments to microscopical stratospheric particles remains an open question.

Here, H<sub>2</sub>O and particle measurements are used to discuss the potential of artificial particle production due to H<sub>2</sub>O contamination. Such artifacts could explain balloon-borne observations of plumes of large particles above the frost point.

### Measurements of H<sub>2</sub>O, T, and particles

The problem of contamination of balloon-borne water vapor measurements due to outgassing of tropospheric water vapor from the balloon and the payload has been known for many years, e.g. from frost point measurements by Mastenbrook [1964] or IR spectrometer measurements by Zander [1966]. In the latter study, during a float of several hours an unexpected increase in humidity was found with increasing solar elevation angle. Zander explained this dependence with a geometric argument, namely that the H<sub>2</sub>O contaminated cloud around the balloon is in the field of view of the instrument only for high elevation angles. Thus the diameter of the H<sub>2</sub>O cloud surrounding the balloon (approximately 30 m diameter at float) could be estimated to be on the order of 100 m. For these reasons, most *in situ* measurements – and not only those of water vapor – are carried out during descent at rates  $> 1 \text{ m/s}$ . Particle measurements, however, have not generally been shown to suffer the same restrictions.

Here we report on massive H<sub>2</sub>O contaminations observed on balloon flights of a balloon-borne Lyman- $\alpha$  fluorescence

<sup>1</sup>Forschungszentrum Jülich GmbH, ICG-I, Jülich, Germany.

<sup>2</sup>University of Wyoming, Laramie, Wyoming, USA.

<sup>3</sup>ETH Zürich, IAC, Zürich, Switzerland.

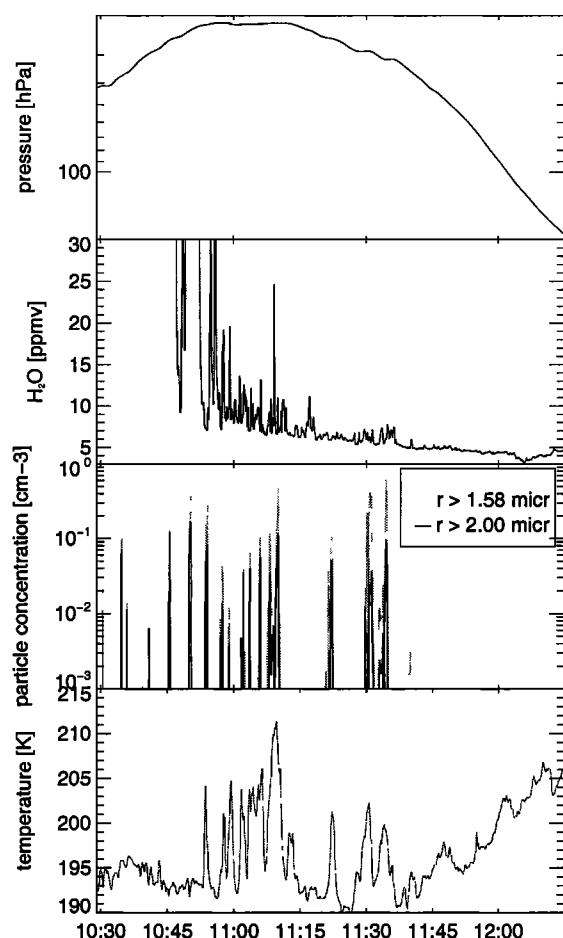


**Figure 1.** Time series of pressure (flight profile),  $\text{H}_2\text{O}$ , particle concentration, and ambient temperature, as measured during the flight on 970211.

hygrometer on 901110 and 970211. The hygrometer [Zöger *et al.*, 1999] was flown in combination with other *in situ* instruments, e.g. a cryogenic whole air sampler. The effect of contamination in air samples taken during ascent has been demonstrated by analyzing for  $\text{H}_2$ , i.e. the balloon filling gas [Schmidt *et al.*, 1991]. The gondolas consist of an open aluminum structure optimized to permit free airflow to the instrument inlets during descent. All instruments are designed to minimize the risk of contamination, e.g. by using exclusively surfaces made of electropolished stainless steel or aluminum. The dimensions of the whole payload are 4 m  $\times$  4 m  $\times$  2 m, the distance between the balloon (size 35,000  $\text{m}^3$  on 901110, 100,000  $\text{m}^3$  on 970211) and the payload is  $\approx$  120 m.

During the first balloon flight of the prototype instrument at midlatitudes on 901110, highly contaminated measurements were obtained during ascent and at float altitude, while descent measurements yielded a typical stratospheric  $\text{H}_2\text{O}$  profile [Mörschel *et al.*, 1991]. The payload was launched under cloudy conditions just before onset of precipitation.  $\text{H}_2\text{O}$  mixing ratios measured during ascent ranged from 20 ppmv when the measurement was started at 21 km (40 hPa) to more than 80 ppmv when the float altitude was reached (7:03 UT). The balloon oscillated at the float level (29 km) with an amplitude of approximately 150 m. Correspondingly, the  $\text{H}_2\text{O}$  signal showed strong peaks up to 160 ppmv in phase with maximum ascent rates during the oscillations. The strength of these peaks decreased during the 35 min float duration. The smaller peaks ( $< 25$  ppmv) at float have been interpreted as contamination from the gondola, while the major peaks have

been attributed to outgassing of the balloon. As soon as a descent rate  $> 2$  m/s was achieved, typical stratospheric mixing ratios of 4–5 ppmv were measured.

On 970211, the hygrometer was part of a balloon payload launched from Kiruna after sunrise. During inflation of the balloon and the launch sequence, moderate snow was falling. The flight was planned to measure atmospheric  $\text{H}_2\text{O}$  profiles during descent. Due to the known problems during ascent, the measurements were started only shortly before reaching float altitude. Figure 1 shows time series of the unfiltered  $\text{H}_2\text{O}$  measurements with 1 Hz sampling frequency. The valve-controlled flight profile can be divided into four regimes: The ascent ( $< 10:56$  UT), the float (10:56–11:13), the slow descent with variable descent rates and periods of short ascents (11:13–11:38), and the descent with rates  $> 2$  m/s ( $> 11:38$ ). After the hygrometer started operation at 10:47, a structured contamination with  $\text{H}_2\text{O}$  abundances between 8 and 80 ppmv was measured. Experience from other balloon and aircraft measurements using this hygrometer show that potential internal contamination of the instrument occurs only for a maximum time of 30–60 s after the valves are opened; therefore, all subsequent signal has to be attributed to the ambient air. At float, measured  $\text{H}_2\text{O}$  mixing ratios show again pronounced features, but at values between 6.5 and 25 ppmv. During the slow first part of the descent, contamination events with a few ppmv are still observed, coinciding with periods of short ascents. The lower envelope can be regarded as the uncontaminated atmospheric mixing ratios (5.2–6.2 ppmv) typical for the polar vortex. The determination of  $2\text{-CH}_4 + \text{H}_2\text{O}$  using  $\text{CH}_4$  data from a whole air sampler yields a constant value consistent with that at lower altitudes [A. Engel and C. Schiller, unpublished results]. During the following descent, there is no indication of contamination, suggesting that the true atmospheric  $\text{H}_2\text{O}$  profile is measured.

Temperature was measured by a thermistor approximately 4 m from the hygrometer outside the gondola. Striking temperature features were observed at the end of the ascent, during float, and slow descent with peak values 5–10 K above the lower envelope (Figure 1). Temperature changes of this magnitude and spatial scales are unlikely to occur in the stratosphere except possibly in breaking lee waves. When measuring air temperature in the vicinity of balloon or equipment at stratospheric pressure, errors of this magnitude are easily superimposed as a result of inappropriate ventilation, or radiation and response time errors [e.g. Ney *et al.*, 1961]. Such phenomena occur primarily at float or during non-constant ascent or descent rates. Thus, it is not surprising that the most pronounced temperature features coincide with changes of the vertical velocity and in several cases with enhanced  $\text{H}_2\text{O}$ .

On 970211, a Wyoming optical particle counter, as used before by Deshler *et al.*, was also included on the gondola. Events of enhanced particle concentrations for sizes up to 2  $\mu\text{m}$ , the maximum detectable size with the counter used on this day, are observed (Figure 1). At float and during descent, they occur exactly when the aforementioned temperature features are observed. During ascent additional particle events are observed, coinciding with adjustments to the balloon ascent rate, but without coinciding temperature enhancement. Spatial inhomogeneities of the contamination and the distance between the instruments might be the reason that not all features coincide for all parameters T, particles and  $\text{H}_2\text{O}$ . The total condensed mass in most particle events peaks near 1 ppmv  $\text{H}_2\text{O}$ . This is below the natural maximum of 4–7 ppmv, which could be expected if the particles were natural. This complicates the analysis of these layers because the identification of the particles as artificial requires simultaneous  $\text{H}_2\text{O}$  measurements. From the condensed mass, and relatively high number concentrations for large particles, we can exclude the

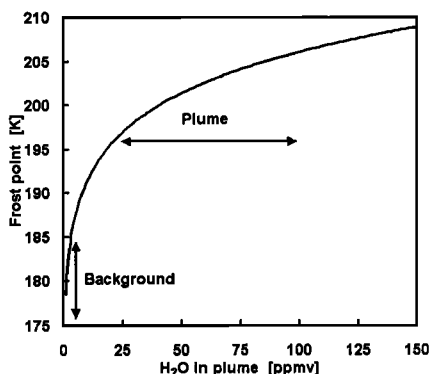


**Figure 2.** Frost point (calculated from *Marti and Mauersberger* [1993]) at 40 hPa versus  $H_2O$  ranging from stratospheric background to values inside contaminated plumes.

possibility that the particles are composed of pure NAT, as observed recently by *Fahey et al.* [2001].

More recent flights of the hygrometer on 990206, 000127, 000301 and 990503 showed very similar events of enhanced  $H_2O$  during ascent, at float and during the early slow descent. So far these measurements were performed on large balloons during daylight, as were the two particle counter flights discussed above. Other particle counter flights on large balloons during the night or on smaller balloons during the day have not displayed these unusual particle events.

## Discussion

The particle measurements on 920127 and on 970211 were performed under similar conditions: same location, season, time of day, and low stratospheric temperatures, around 195 K, but significantly above the frost point; however, the flight on 920127 was launched under clear sky while 970211 under snowfall. Dimensions and configuration of the flight train and the balloon as well as ascent rates were comparable up to 18–20 km. Above this point the flight profiles differed slightly as the balloon ascent rates were slowed.

Comparing the features observed on both flights, there are a number of similarities. Both data sets show events with rapidly changing particle sizes and/or  $H_2O$ , which could be interpreted as ultrafine layers whose vertical extension is on the order of the descent rate divided by the sampling frequency or even lower. During both flights several particle events are characterized by temperatures enhanced by 5–10 K above temperatures at neighboring altitudes. Due to the above-mentioned artifacts of temperature measurements, *Deshler et al.* classify the large temperature fluctuations observed on 920127 as spurious. There are, however, two differences between the temperature measurements on the two days. On 920127 the strong temperature oscillations begin during ascent, well below ceiling, and fluctuations in the ascent rate suggested several strong temperature inversions above 20 km. This suggests real atmospheric temperature perturbations, which *Deshler et al.* took as indicative of mountain waves being the origin of the observed particles. For the flight on 970211 under conditions without mountain-wave perturbations, the temperature features between the end of the ascent and the steady descent must be classified as erroneous, and the spurious temperature fluctuations may be related to the lower and more oscillatory ascent rate and/or differences in gondola configuration.

Ascent rates during the large particle events on 920127 were 1–4 m/s with only a few lower exceptions. Under such conditions water vapor contamination can originate from the balloon skin carrying  $H_2O$  from the tropopause as suggested

by *Zander* [1966], from  $H_2O$  traces in the balloon filling gas, or from the payload itself. An unambiguous identification of the source for the observed contamination events is hardly possible based on available data.

Considering an ascent rate of 3–5 m/s and the distance between the payload and the center of the balloon of approximately 150 m,  $H_2O$  contamination from the balloon skin could generate large supersaturations with subsequent formation and growth of ice particles, which may be detected 30–50 s later by the payload. The contamination could be caused by  $H_2O$  evaporating from the balloon skin, for example when the solar heating of a skin segment changes after a rotation. This may generate massive supersaturations when the  $H_2O$ -enriched air cools upon mixing with cold ambient air. Such a contamination could either by itself be discontinuous, or it could be detected intermittently due to vertical wind shear causing oscillations of the gondola, and therefore could appear as particle micro-layers at the payload's altitude.

The gas filling of the balloon could also be the source of  $H_2O$  enriched plumes. The  $H_2$  used is specified to contain a  $H_2O$  mixing ratio of less than 20 ppmv by the supplier (AGA Gas AB). Again, this could lead to layer-like particle events at the altitude of the payload when either gas is released during a balloon maneuver or when the particles sediment out of the gas filling after adiabatic cooling. Due to adiabatic expansion, the temperature inside the balloon is lower by 5–10 K than ambient temperature during ascent. Thus, formation of ice particles in the balloon gas itself is likely. During the 30 min ceiling, the gas temperature approaches the ambient temperature, and during descent it becomes warmer than the surrounding air by up to 30 K. These observations are similar for other balloon flights including that of 920127.

It is, however, much less clear how ice particles formed within the balloon would exit the balloon envelope except during a balloon maneuver, when the valve at the top of the balloon is open. The balloons used were open at the base with a duct; however, this duct is effectively open only close to ceiling altitudes when the balloon is fully inflated. The particle events on 920127 began during ascent at 40 hPa, well below the ceiling, and could not be associated with balloon maneuvers, while those on 970211 could be closely associated with balloon maneuvers, i.e. changes in ascent rate.

Both the  $H_2O$  measurements, and consideration of the balloon environment, suggest that contamination will most likely occur through outgassing of  $H_2O$  from either the balloon envelope or filling gas. In this case thermodynamic and

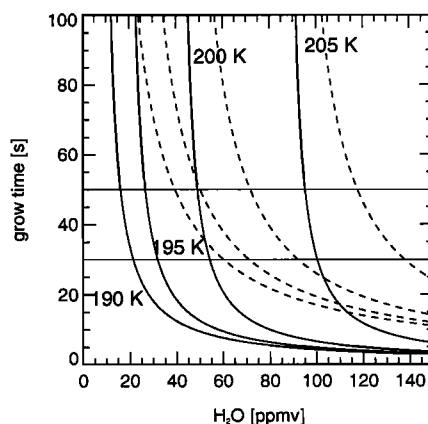


**Figure 3.** Time required for ice crystals to grow to 2  $\mu\text{m}$  (solid lines) and 5  $\mu\text{m}$  (dashed lines) radius versus  $H_2O$  at 40 hPa for different temperatures. Horizontal lines mark the period from the emission from the balloon until the gondola reached the plume.

kinetic conditions would then support the development of large particles. The observed water mixing ratios of 10–80 ppmv imply significantly higher frost points than those given by undisturbed stratospheric mixing ratios of 4–6 ppmv. Figure 2 shows these frost points at 40 hPa ambient pressure as a function of the  $\text{H}_2\text{O}$  mixing ratio  $\chi$ . At  $\chi = 80$  ppmv the frost point reaches 205 K. Under such conditions the stratospheric background particles ( $\text{H}_2\text{SO}_4/\text{H}_2\text{O}$  droplets) will take up water and freeze as water ice particles within a fraction of a second. However, the subsequent growth process is much slower, hence rapid nucleation alone does not guarantee that the ice crystals reach the large radii  $r > 5 \mu\text{m}$  as observed.

The time  $\tau$  required for ice particles after nucleation to grow to a radius  $r$  can be estimated from  $r \cdot dr/dt = \beta \cdot (S-1)$ , where  $S = p_{\text{H}_2\text{O}}/p_{\text{H}_2\text{O}}^{\text{ice}}$  is the saturation ratio of water with respect to ice, with water partial pressure in the contamination plume  $p_{\text{H}_2\text{O}}$  and temperature-dependent water vapor pressure over ice  $p_{\text{H}_2\text{O}}^{\text{ice}}$ . An approximate expression for the growth factor [Peter et al., 1994] is  $\beta = 1.3 \cdot 10^4 \mu\text{m}^2/\text{s} \cdot (\chi/S) (T/190\text{K})^{1/2} / (1 + 1.6 \mu\text{m}/r)$ . Assuming  $\chi$  and  $T$  to remain constant during growth process, the growth law can be integrated to yield the growth time

$$\tau \approx 3.8 \cdot 10^{-5} \text{ s} \cdot \frac{1}{\chi} \cdot \frac{S}{S-1} \cdot \left( \frac{190 \text{ K}}{T} \right)^{1/2} \cdot \frac{r}{\mu\text{m}} \cdot \left[ \frac{r}{\mu\text{m}} + 3.2 \right]$$

A high  $\text{H}_2\text{O}$  mixing ratio  $\chi$  helps the ice crystals to grow to large radii even within the 30–50 s available between the release of a contaminated plume at the balloon and its detection by the instruments. Figure 3 shows typical growth times for ice crystals to reach  $r = 5 \mu\text{m}$  as observed on 920127 (dashed lines) according to the growth time equation. At 190–195 K,  $\chi \approx 40$ –75 ppmv may generate  $5 \mu\text{m}$  particles within the 30–50 s time lag.  $\chi \approx 15$ –30 ppmv is required for particles to grow within the same time to  $r = 2 \mu\text{m}$  as observed on 970211 (Figure 3 solid lines). This range of  $\text{H}_2\text{O}$  and  $T$  covers the observations in the contaminated plumes. At 205 K,  $\chi < 100$  ppmv does not suffice for particle growth.

Alternatively, the payload itself could be the source of the contamination, but this is unlikely. Ascent rates of even  $1$ – $2 \text{ m s}^{-1}$  would not allow vapor emitted by the gondola to be re-sampled as particles after 30–50 s. The particles might also have been formed already on the moist balloon skin or the payload, and could be occasionally released due to mechanical stress on the skin or changing illumination by the sun if the balloon were rotating. They evaporate rapidly (the same equation as for the growth rate is applicable) and moisten the nearby air. Nevertheless, they survive before they are reached by the payload if their original size is large, say  $r \geq 30 \mu\text{m}$ .

## Summary and conclusions

Simultaneous balloon-borne  $\text{H}_2\text{O}$ , temperature and particle measurements suggest that artificial ice particle production can occur at temperatures around 200 K, well above the ambient frost point, due to  $\text{H}_2\text{O}$  contaminations on the order of 25–100 ppmv. The observed  $\text{H}_2\text{O}$  and particle enhancements appear in short-lived events, which could be explained in terms of bursts of  $\text{H}_2\text{O}$  emission from the balloon skin or filling gas. In these events the condensed particulate mass was near  $1.0 \text{ ppmv H}_2\text{O}$ . Since condensed  $\text{H}_2\text{O}$  masses of a few ppmv can occur in a typical stratospheric ice cloud, the interpretation of such particle layers is complicated and suggests the need for coincident  $\text{H}_2\text{O}$  measurements. Artificial particle production in the wake of balloons will not occur at  $T > 205 \text{ K}$ , since even for 100 ppmv  $\text{H}_2\text{O}$  the air remains unsaturated with respect to ice. For observations in darkness the

degree of desorption from the balloon skin is lower in the absence of sun light heating the surfaces. Contamination is also unlikely to affect measurements during descent at rates  $> 2 \text{ m/s}$  independent of temperature or sun light conditions.

These measurements could also explain some observations in the past which were interpreted as particle micro-layers at temperatures above the frost point. Natural mechanisms for extending the existence of ice particles to temperatures above the frost point, such as NAT-coating, have been suggested as possible explanation in several microphysical studies in the past. Recent laboratory studies, however, do not corroborate this idea, and the experimental evidence for such a phenomenon has diminished with our study.

**Acknowledgements.** We acknowledge discussions with M. Helten, U. Schmidt, D. McKenna, and the staff of CNES and ESRANGE.

## References

- Biermann, U. M., et al., FTIR studies on lifetime prolongation of stratospheric ice particles due to NAT coating, *Geophys. Res. Lett.*, **25**, 3939–3942, 1998.
- Deshler, T., T. Peter, R. Müller, and P. Crutzen, The lifetime of lee-wave-induced ice particles in the Arctic stratosphere: I. Balloon-borne observations, *Geophys. Res. Lett.*, **21**, 1327–1330, 1994.
- Fahey, D. W., et al., The detection of large  $\text{HNO}_3$ -containing particles in the winter Arctic stratosphere, *Science*, **291**, 1026, 2001.
- Goodman, J., S. Verma, R. F. Pueschel, P. Hamill, G. V. Ferry, D. Webster, New evidence of size and composition of polar stratospheric cloud particles, *Geophys. Res. Lett.*, **24**, 615–618, 1997.
- Hofmann, D. J., and T. Deshler, Comparison of stratospheric clouds in the Antarctic and the Arctic, *Geophys. Res. Lett.*, **16**, 1429–1432, 1989.
- Hofmann, D. J., Stratospheric cloud micro-layers and small scale temperature variations in the Arctic in 1989, *Geophys. Res. Lett.*, **17**, 369–372, 1990.
- Khattatov, V., et al., Some results of  $\text{H}_2\text{O}$ , ozone and aerosol measurements during EASOE, *Geophys. Res. Lett.*, **21**, 1299, 1994.
- Marti, J. and K. Mauersberger, A survey and new measurements of ice vapor pressure at temperatures between 170 and 250 K, *Geophys. Res. Lett.*, **20**, 363–366, 1993.
- Mastenbrook, H. J., Frost point hygrometer measurements in the stratosphere and the problem of moisture contamination, *Humidity and Moisture*, **2**, ed. E. J. Amdur, 480–485, Reinhold Publ. Corp., New York, 1964.
- Middlebrook, A. M., and M. A. Tolbert, Evaporation studies of model polar stratospheric cloud films, *Geophys. Res. Lett.*, **23**, 2145–2148, 1996.
- Mörschel, U., E. Klein, D. Kley, and U. Schmidt, A new balloon borne stratospheric hygrometer, *Proc. 10th ESA Symp., ESA SP-317*, 201–205, 1991. Available via [http://www.fz-juelich.de/icg/icg1/publications/Sonstiges/sonstiges\\_e.html](http://www.fz-juelich.de/icg/icg1/publications/Sonstiges/sonstiges_e.html)
- Ney, E. P., R. W. Maas, and W. F. Huch, The measurement of atmospheric temperature, *J. Meteorol.*, **18**, 60–80, 1961.
- Peter, T., R. Müller, P. Crutzen, T. Deshler, The lifetime of lee-wave-induced ice particles in the Arctic stratosphere: II. Stabilization due to NAT-coating, *Geophys. Res. Lett.*, **21**, 1331–1334, 1994.
- Schmidt, U., et al., Profile observations of long-lived trace gases in the Arctic vortex, *Geophys. Res. Lett.*, **18**, 767–770, 1991.
- Zander, R., Moisture contamination at altitude by balloon and associated equipment, *J. Geophys. Res.*, **71**, 3775–3778, 1966.
- Zöger, M. et al., Fast in situ stratospheric hygrometers: A new family of balloonborne and airborne Lyman- $\alpha$  photofragment fluorescence hygrometers, *J. Geophys. Res.*, **104**, 1807–1816, 1999.
- C. Schiller, Forschungszentrum Jülich, ICG-I, 52425 Jülich, Germany. (e-mail: c.schiller@fz-juelich.de)
- T. Deshler, Department of Atmospheric Sciences, University of Wyoming, Laramie, WY 82071, USA. (e-mail: deshler@uwyo.edu)
- T. Peter, ETH Zürich, IAC, Hoenggerberg HPP L8.2, 8093 Zürich, Switzerland. (e-mail: thomas.peter@ethz.ch)

(Received: April 5, 2001; revised: July 6, 2001; accepted: July 8, 2001)